NUMERICAL SIMULATION OF THE ONSET OF UNSTEADY FLOW IN NATURAL CONVECTION LOOPS

Samuel Wakefield[1], Milan Mihajlović[1*]

[1]Department of Mechanical, Aerospace and Civil Engineering, University of Manchester, Manchester M13 9PL, United Kingdom

1. INTRODUCTION

Natural convection loops appear in numerous passive heat exchange systems, one example being the safety systems in nuclear reactors cooling. The fluid flow is driven by thermal gradients between hot and cold regions and exhibits complex dynamical behaviour when these gradients are increased. In this study we report on the numerical simulation results for the onset of unsteady flow in natural convection loops. Our preliminary findings suggest that the mechanisms of transition to unsteady flow in loops are more complex than those observed in rectangular cavities.

2. MATHEMATICAL MODEL AND DISCRETISATION

The natural convection flows are modelled by the Boussinesq approximation of the Navier-Stokes equations (see Elman et al. [1, Chapter 11]). We adopt the non-dimensionalisation suggested in Christon et al. [2], with the characteristic length scale L_*, velocity scale $U_* = \sqrt{g\beta L_* \Delta T}$, time scale $\tau_* = \frac{L_*}{U_*}$, and pressure $P_* = \rho U_*^2$, where $\Delta T = T_h - T_c$ is the temperature difference between hot and cold sections, g the gravity constant, and β the fluid volume expansion coefficient. Then, the Boussinesq system for the unknown fluid velocity $\boldsymbol{u}$, pressure p, and temperature T reads:

$$\frac{\partial \boldsymbol{u}}{\partial t} - \epsilon_u \Delta \boldsymbol{u} + \boldsymbol{u} \cdot \nabla \boldsymbol{u} + \nabla p = \boldsymbol{g} T \quad \text{in } W = \Omega \times [0, \tau] \tag{1}$$

$$\nabla \cdot \boldsymbol{u} = 0 \qquad \text{in } \Omega \tag{2}$$

$$\frac{\partial T}{\partial t} - \epsilon_T \Delta T + \boldsymbol{u} \cdot \nabla T = 0 \qquad \text{in } W \tag{3}$$

The viscosity parameters ϵ_u and ϵ_T are expressed in terms of the Rayleigh number Ra and the Prandtl number Pr as $\epsilon_u = \sqrt{\frac{Pr}{Ra}}$ and $\epsilon_T = \frac{1}{\sqrt{Pr \cdot Ra}}$, where $Ra = \frac{g\beta\Delta T L^3}{\mu\alpha}$, $Pr = \frac{\mu}{\alpha}$ (μ is the molecular diffusivity and α the thermal diffusion coefficient). The system (1)-(3) is augmented with a set of standard boundary conditions, i.e., the no-slip velocities on all walls

$$\boldsymbol{u} = \boldsymbol{0} \qquad \text{on } \partial\Omega \times [0, \tau] \tag{4}$$

and adiabatic temperature conditions on all walls ($\partial\Omega_N^T$)

$$\epsilon_T \nabla T \cdot \hat{\boldsymbol{n}} = 0 \qquad \text{on } \partial\Omega_N^T \times [0, \tau] \tag{5}$$

except on the walls of the hot (the subscript h) and the cold section (the subscript c) (collectively denoted by $\partial\Omega_D^T$), where inhomogeneous Dirichlet boundary conditions are imposed:

$$T_h = \frac{1}{2}(1 - e^{-\gamma t}), \qquad T_c = -\frac{1}{2}(1 - e^{-\gamma t}) \tag{6}$$

In (5) $\hat{\boldsymbol{n}}$ denotes the outward pointing unit normal vector at every point of the boundary $\partial\Omega_N^T$. The exponential term in (6) ensures gradual heating and cooling of the hot and the cold walls respectively. This scenario is closer to the physical reality than the impulse start, and avoids any spurious oscillations in the numerical solution.

The time discrerisation deployed in this context is trapezoid rule, which has asymptotic second-order accuracy. The time interval of interest $[0, \tau]$ is divided into N_τ subintervals of variable size. After time discretisation the semi-discrete problem (1)-(3) reads: given the approximations $(\boldsymbol{u}^{[n]}, p^{[n]}, T^{[n]})$ at time $t_n,\ n = 0,1, \ldots N_\tau$ and the boundary data $T_h^{[n+1]}$and $T_c^{[n+1]}$, compute $(\boldsymbol{u}^{[n+1]}, p^{[n+1]}, T^{[n+1]})$ via

$$\frac{2}{\Delta t_{n+1}}\boldsymbol{u}^{[n+1]} - \epsilon_u \Delta \boldsymbol{u}^{[n+1]} + \boldsymbol{u}^{[n++]} \cdot \nabla \boldsymbol{u}^{[n+1]} + \nabla p^{[n+1]} - \boldsymbol{g}T^{[n+1]} = \frac{2}{\Delta t_n}\boldsymbol{u}^{[n]} + \frac{\partial \boldsymbol{u}^{[n]}}{\partial t} \quad \text{in } \Omega \qquad (7)$$

$$-\nabla \cdot \boldsymbol{u}^{[n+1]} = 0 \quad \text{in } \Omega \qquad (8)$$

$$\frac{2}{\Delta t_{n+1}}T^{[n+1]} - \epsilon_T \Delta T^{[n+1]} + \boldsymbol{u}^{[n+1]} \cdot \nabla T^{[n+1]} = \frac{2}{\Delta t_n}T^{[n]} + \frac{\partial T^{[n]}}{\partial t} \quad \text{in } \Omega \qquad (9)$$

In (7)-(9) $\Delta t_{n+1} = t_{n+1} - t_n$ is the current step, $\frac{\partial u^{[n]}}{\partial t} = \epsilon_u \Delta \boldsymbol{u}^{[n]} - \boldsymbol{u}^{[n]} \cdot \nabla \boldsymbol{u}^{[n]} - \nabla p^{[n]} + \boldsymbol{g}T^{[n]}$ is the fluid acceleration at t_n, and $\frac{\partial T^{[n]}}{\partial t} = \epsilon_T \Delta T^{[n]} - \boldsymbol{u}^{[n]} \cdot \nabla T^{[n]}$ is the rate of change in temperature at t_n.

The standard trapezoid rule is stabilised using time averaging technique [6], which is applied periodically. This circumvents the problem of locking the time step size in adaptive setting, which is caused by the lack of damping in the standard algorithm. We use adaptive time steps in the simulation, with the step size selection done via a predictor-corrector scheme, using the AB2 method as a predictor [7].

The semi-discrete problem (7)-(9) is non-linear and a numerical scheme for its linearization is required. Standard approaches used in this context are Picard's or Newton's linearization. These techniques can achieve arbitrary level accuracy, but are computationally expensive, requiring multiple solutions of large, sparse linear systems at every time step. An alternative approach is to extrapolate $\boldsymbol{u}^{[n+1]}$ using the second-order accurate approximation

$$\boldsymbol{u}^{[n+1]} \approx \left(1 + \frac{\Delta t_{n+1}}{\Delta t_n}\right)\boldsymbol{u}^{[n]} - \frac{\Delta t_{n+1}}{\Delta t_n}\,\boldsymbol{u}^{[n-1]} \qquad (10)$$

In this way the resulting numerical scheme retains its asymptotic order of accuracy, while being much simpler and computationally cheaper, requiring only the solution of a single linear system per time step. Notice, however, that for tight tolerances the numerical schemes based on Picard's and Newton's linearization are more accurate in absolute terms.

Finally, the semi-discrete problem (7)-(9) with the linearization (10) is discretised in space using a method of lines based on finite element approximation over a fixed grid of quadrilateral elements. We use the inf-sup stable Taylor-Hood method (Q2-Q1), with the continuous biquadratic approximation for the velocity components and the continuous bilinear approximation for pressure. The temperature is discretised by biquadratic approximation (Q2), which is the approach suggested in the literature [8].

The sparse linear systems that arise in this context can be solved either by a direct sparse solver, or by a Krylov iterative method. A tailor-made block preconditioner for the latter case is developed in [3]. In this work we solve the systems using a direct method. The implementation of the described method is done in MATLAB as part of the IFISS finite element library [4].

3. NUMERICAL RESULTS

We consider the same loop geometry that was studied by Wilson et al. in [5] (see Fig. 1). The length and the height of the straight segments in the loop are equal to 6, and the channel diameter is 1. The inner radius of straight-angled bends is equal to 1.5. The hot segment (depicted in red) of length 3.5 is placed symmetrically at the bottom straight segment, and the cold segment (depicted in blue) of the same length occupies the top of the right vertical segment.

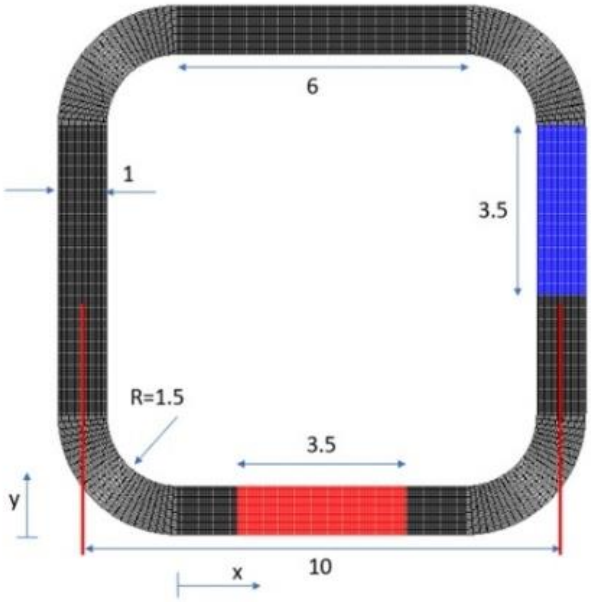

Figure 1: The loop domain geometry with the parameters and a sample finite element grid. The hot segment is depicted in red and the cold segment in blue.

We simulate the flow of air ($Pr = 0.71$) and consider a range of Ra between 100,000 and 300,000. The simulation is performed over a long interval ($\tau = 1000$), thus ensuring that the initial transient behaviour is damped, and that we can study the system's asymptotic behaviour.

3.1 Convergence tests

We study the consistency and accuracy of the results across two different finite element grids. In this experiment we consider two values of Ra (100,000 and 150,000). The coarse grid has 122,430 degrees of freedom, and the fine grid 316,200 degrees of freedom. There are 35 elements across the channel in the coarse grid and 40 elements in the fine grid. In the case $Ra = 100{,}000$ the solution is steady, while for $Ra = 150{,}000$ we observe small pulsating variations (see Fig. 2.a) In both cases we compare the average values of the velocity components u_x and u_y, and temperature T. In addition, for $Ra = 150{,}000$ the magnitude of oscillations in these quantities is reported. The results are summarised in Table 1 for $Ra = 100{,}000$ and in Table 2 for $Ra = 150{,}000$.

The results look consistent in both cases, with only minor differences which are of order 10^{-4}. In the remaining simulations we use only the fine grid with 316,200 degrees of freedom. Further validation of

these results should involve the comparisons with a numerical scheme in which the solution of the non-linear problem done by Picard's or Newton's iteration.

Table 1: The steady-state values of the velocity components u_x and u_y, and temperature T for $Ra = 100{,}000$ and two different discrete problem sizes n.

n	u_x	u_y	T
122,430	-0.7870	0.0013	-0.1109
316,200	-0.7868	0.0013	-0.1110

Table 2: The average values and the magnitudes of oscillations of the velocity components u_x and u_y, and temperature T for $Ra = 150{,}000$ and two discrete problem sizes n.

n	$\overline{u_x}$	Δu_x	$\overline{u_y}$	Δu_y	$\bar{T}$	ΔT
122,430	-0.7241	0.0006	0.0004	0.0009	-0.0988	0.0002
316,200	-0.7239	0.0006	0.0004	0.0009	-0.0989	0.0002

3.2 The onset of the time-dependent flow

We perform a set of simulations for four different values of Ra. The time step sizes selected by the adaptive integrator vary in the asymptotic regime between 0.4 for $Ra = 150{,}000$ and 0.09 for $Ra = 300{,}000$ (the integration over the interval $[0{,}1000]$ took 4223 steps in the former and 12591 steps in the latter case).

The flow appears laminar for $Ra = 100{,}000$, but for larger values we observed a transition to a non-steady regime. In laterally heated rectangular cavities the transition to a non-steady flow is via a simple Hopf bifurcation, with a pair of complex eigenvalues crossing from the left (stable) to the right (unstable) half of the complex plane at the critical value of Ra. This results in a simply-periodic oscillatory flow [2]. By contrast, the transition to unsteady flow in convective loops exhibits a more complex pattern. In Fig. 2 we present the traces of the horisontal velocity u_x at the point $(0, -5)$, which lies in the centre of the hot section, and in Fig. 3 the traces of temperature for $Ra = 250{,}000$ and $Ra = 300{,}000$. The traces exhibit periodic behaviour, but their shape suggests the presence of multiple harmonics in the signal. We perform the Fourier analysis of the computed signals in MATLAB. For the two lower values of Ra (150,000 and 200,000) the Fourier spectrum is broad, without clear peaks, while in the cases $Ra = 250{,}000$ and 300,000 we detect 2-3 sharp peaks in the spectrum, indicating a small number of unstable complex eigenvalues. These preliminary findings warrant a more detailed study and verification by more accurate numerical techniques, including the turbulence models [5].

Finally, in Fig. 4 we plot the isotherms in the bottom horisontal section of the loop at time $t = 975$ for $Ra = 300{,}000$. This time instance corresponds to the local temperature peak at the control point $(0, -5)$. The figure depicts a complex, non-symmetric temperature distribution.

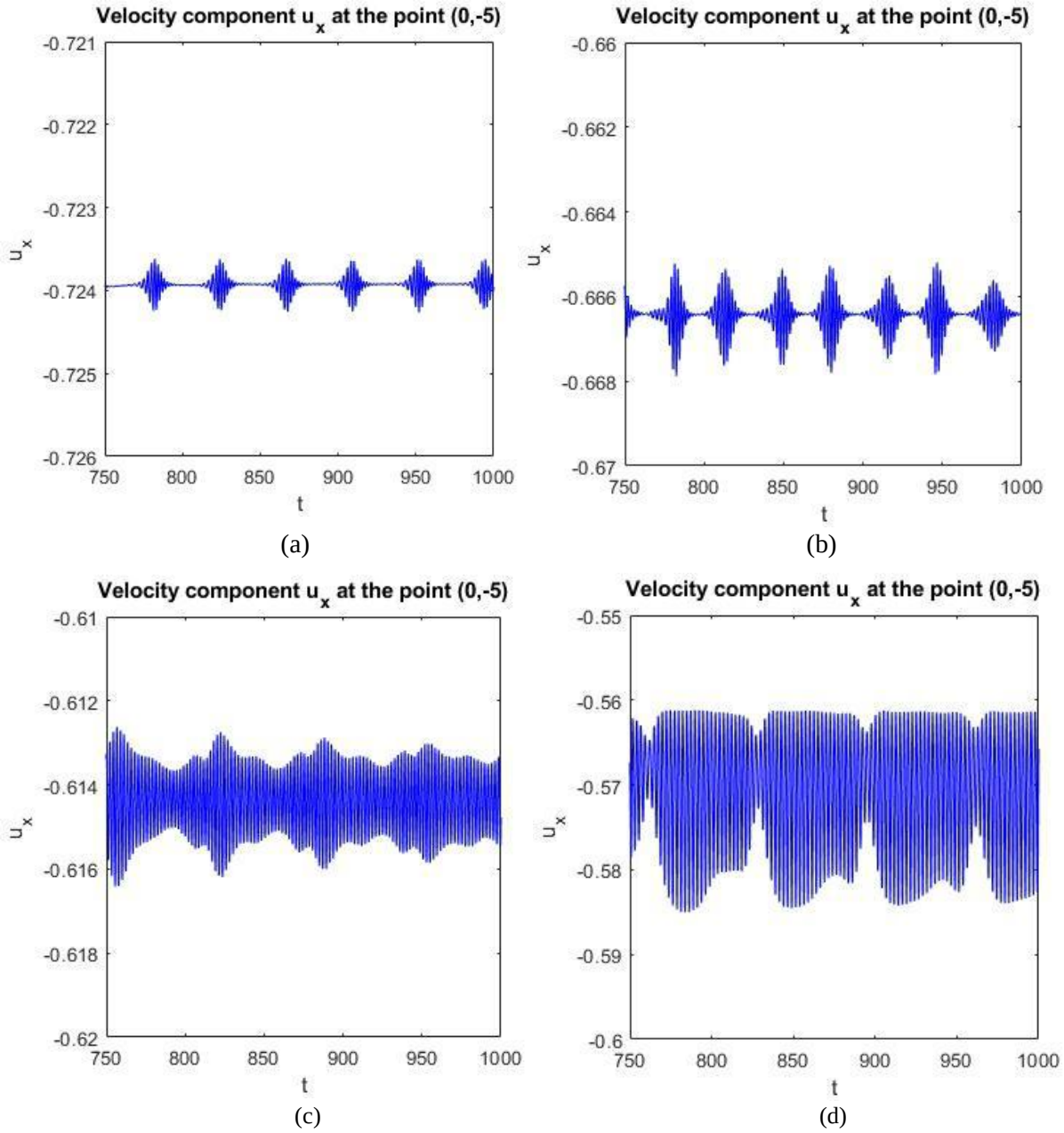

Figure 2: Velocity component u_x traces at the middle point of the hot area $(0, -5)$:
(a) $Ra = 150{,}000$, (b) $Ra = 200{,}000$, (c) $Ra = 250{,}000$, (d) $Ra = 300{,}000$.

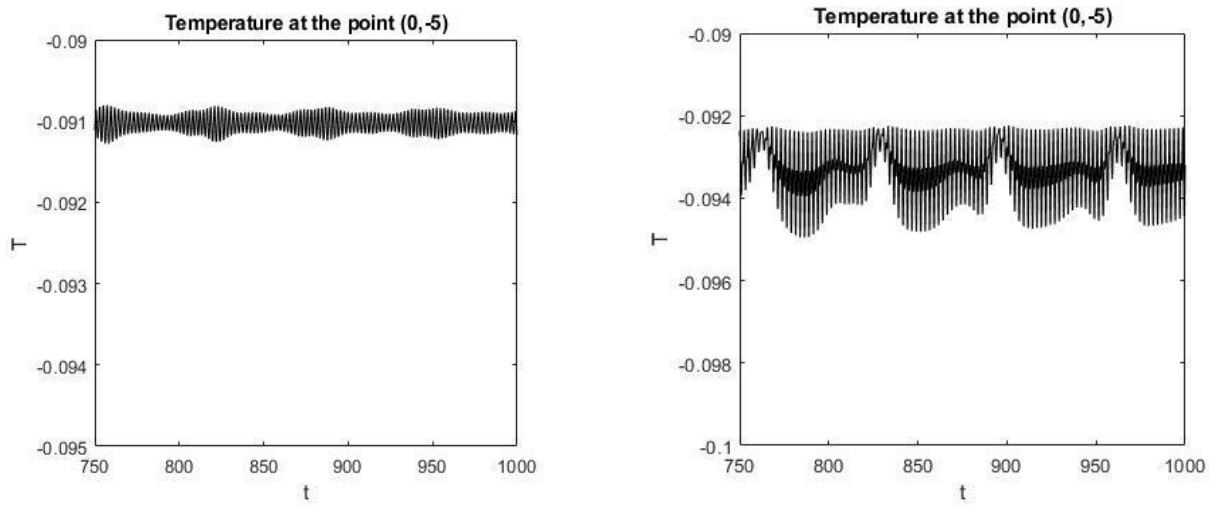

(a) (b)

Figure 3: Temperature traces at the middle point of the hot area $(0, -5)$:
(a) $Ra = 250{,}000$, (b) $Ra = 300{,}000$.

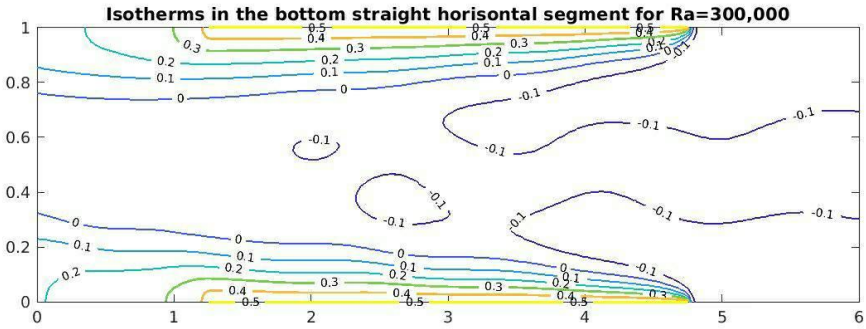

Figure 4: The isotherms in the bottom straight segment of the cavity at $t = 975$ for $Ra = 300{,}000$.

REFERENCES

1. H. Elman, D. Silvester, A. Wathen, *Finite Elements and Fast Iterative Solvers with Applications in Incompressible Fluid Dynamics*, 2nd ed., Oxford University Press, 2014.
2. M.A. Christon, P.M. Gresho, S.B. Sutton, Computational predictability of time-dependent natural convection flows in enclosures (including a benchmark solution), *Int. J. Numer. Methods Fluids* **40** (2002), 953–980.
3. H. Elman, M. Mihajlović, D. Silvester, Fast iterative solvers for buoyancy driven flow problems, *J. Comput. Phys.*, **230** (2011), 3900-3914.
4. H. C. Elman, A. Ramage, D. J. Silvester, IFISS: A computational library for investigating incompressible flow problems, *SIAM Rev.*, **56** (2014), 261-273.
5. D. Wilson, H. Iacovides, T. Craft, Numerical Insights into the Transient Behaviour of Single Phase Natural Convection Loops for Nuclear Passive Cooling Applications, *Proc. 11th International Symposium on Turbulence and Shear Flow Phenomena*, Southampton, 2019.
6. D.A. Kay, P.M. Gresho, D.F. Griffiths, D.J. Silvester, Adaptive time-stepping for incompressible flow; part II: Navier–Stokes equations, *SIAM J. Sci. Comput.*, **32** (2010) 111–128.
7. P.M. Gresho, R.L. Sani, Incompressible Flow and the Finite Element Method, Isothermal Laminar Flow, vol. 2, John Wiley, Chichester, 2000.
8. M.D. Gunzburger, Finite Element Methods for Viscous Incompressible Flows, Academic Press, London, 1989.